

# Coulomb Crystals in a Pulse-Excited Linear Paul Trap

N. Kjærgaard, K. Mølhave, and M. Drewsen

*Institute of Physics and Astronomy, Aarhus University, DK-8000 Aarhus C, Denmark*

**Abstract.** We present results from recent experiments with laser cooled  $^{24}\text{Mg}^+$  ions captured in a pulse-excited linear Paul trap. As discussed in [1–3], the radial/transverse dynamics of charged particles in an electric quadrupole trap with a pulsed voltage excitation is analogous to that of particles travelling through the alternating gradient (AG) magnetic quadrupole lattice of a storage ring or transport channel. Hence, the pulse-excited Paul quadrupole trap may be used to emulate non-neutral beam propagation. In a series of experiments, we have investigated the stability of stationary Coulomb crystals. The results comply with current theory of crystalline plasmas and beams. We observe, however, that the plasma may stay crystalline beyond the expected stability region in a hitherto unseen configuration consistent with a string of rotating discs.

## INTRODUCTION

When a charged particle travels through a magnetic quadrupole it experiences a focusing force in one dimension and a defocusing force in the perpendicular dimension. However, by combining two quadrupoles with opposite polarities into a doublet a net focusing effect can be obtained in both dimensions as illustrated in Fig. 1. Alternating gradient (AG) magnetic quadrupole focusing was proposed by Courant, Livingston, and Snyder [4] in the early 1950's<sup>1</sup> and despite its simplicity, this concept revolutionized accelerator design [6] and is today widely used in storage rings to achieve transverse confinement of particles along the design orbit. The resulting transverse dynamics can be emulated in the stationary frame of an electric quadrupole trap [1–3] and in recent experiments we have exploited this analogy to investigate the stability of laser cooled  $^{24}\text{Mg}^+$  Coulomb crystals produced and imaged as described in [7].

## THE PULSE-EXCITED LINEAR PAUL TRAP

The linear Paul trap employed in the experiments consists of four cylindrical electrodes, as shown in Fig. 2(a), with a radius of  $R = 4.0$  mm; the radius of the inscribed inter-electrode space is  $r_0 = 3.5$  mm. To operate the trap in a pulsed mode, the periodic rf voltage  $\phi_\tau(t)$  shown in Fig. 2(b) is applied to the rods. The pulsed waveform is characterized by an amplitude  $V_{\text{rf}}$ , a period  $T$ , and a pulse duration  $\tau T$ . As indicated

---

<sup>1</sup> The idea had been suggested earlier by Christofilos [5] but was unpublished.

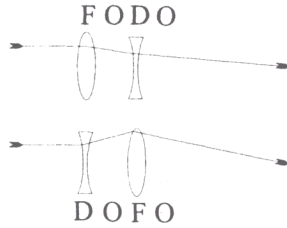


**FIGURE 1.** Principle of AG focusing. A focusing-defocusing or defocusing-focusing lens pair gives rise to net focusing. For equally strong lenses the inter-lens distance should be less than twice the magnitude of the lens focal length. The combination 'Focusing (F)-Drift (O~"zero")-Defocusing (D)-Drift (O~"zero")' is commonly referred to as a *FODO cell*.

in Fig. 2(a), the pulses are applied alternately (  $\begin{pmatrix} \oplus\oplus \\ \ominus\ominus \end{pmatrix} / \begin{pmatrix} \ominus\ominus \\ \oplus\oplus \end{pmatrix}$  ) to the two pairs of diagonally opposite quadrupole rods with a phase delay of  $T/2$ . The resulting voltage difference between adjacent rods then varies as shown in Fig. 2(c). The time-dependent electric potential near the axis approximates a perfect quadrupole

$$\Psi_p(x, y, t) = \frac{\phi_\tau(t) - \phi_\tau(t - T/2)}{2} \frac{x^2 - y^2}{r_0^2}, \quad (1)$$

and gives rise to pseudo-harmonic radial confinement. The corresponding radial oscillation frequency  $\omega_p$  can be calculated from the one period transfer matrix [3, 8]. In Eq. (1), the time elapsed between subsequent focusing and defocusing pulses is  $T/2$  and all pulses have the same duration and amplitude. For an energetic ion beam in a magnetic AG storage ring, this corresponds to propagation through a regular so-called

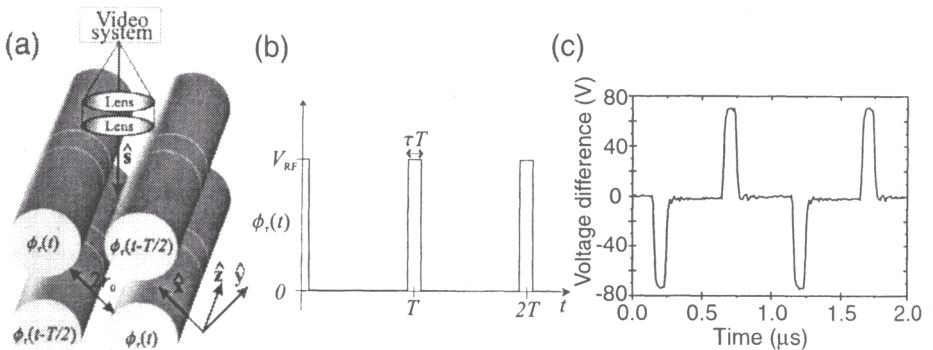


**FIGURE 2.** (a) The linear Paul trap. Time-varying voltages  $\phi_\tau(t)$  and  $\phi_\tau(t - T/2)$  are applied to adjacent rods as shown. To obtain axial confinement of ions, each electrode is sectioned into three and an additional dc voltage  $U_{dc}$  is applied to the eight end-pieces with respect to the center-pieces. (b) The pulsed, time-varying waveform  $\phi_\tau(t)$ . (c) Example of the measured time-varying voltage differences between adjacent quadrupole rods when the dual channel pulse amplifier applies voltage pulses alternately to the two pairs of diagonally opposite quadrupole rods;  $\omega_{RF} = 2\pi \times 1$  MHz and pulse duration 100 ns (i.e.,  $\tau = 0.1$ ).

FODO-lattice<sup>2</sup>. The parameters can, however, be varied quite arbitrarily with respect to duration and delay and still give rise to radial confinement. The pulses are produced by a dual-channel pulse amplifier with inputs from two pulse generators triggered at the desired repetition frequency by a function generator. Each channel of the pulse amplifier is rated to a pulse amplitude of 200 V at  $\omega_{RF} = 2\pi \times 1$  MHz with a minimum pulse duration  $< 100$  ns. An axial confinement force is achieved by sectioning each of the quadrupole rods into three as shown in Fig. 2(a) and applying an additional dc voltage  $U_{dc}$  to the eight end-pieces. This gives rise to a static, approximately harmonic potential  $\Psi_s(x, y, z) = \eta z_0^{-2} U_{dc} [z^2 - (x^2 + y^2)/2]$ , where  $\eta$  is a geometric factor. In the current experiments,  $z_0 = 5.4$  mm corresponding to  $\eta = 0.248$  and the harmonic approximation is valid up to a few millimeters from the trap center. The single particle axial oscillation frequency is  $\omega_z = \sqrt{-a/2} \omega_{rf}$ , where  $a = -4\eta e U_{dc} / m z_0^2 \omega_{rf}^2$ . We note that the axially confining force arising from the static potential  $\Psi_s$  is accompanied by a radial, defocusing force. Denoting the radial distance to the trap axis by  $\rho$  the radial component of this force is  $F_{s,\rho} = m(\omega_z^2/2)\rho$ .

### Cold Plasma in a Harmonic Trap

The linear Paul trap can be described as a harmonic trap with an effective potential of the form (using cylindrical coordinates)

$$\Phi(\mathbf{r}) = \frac{m\omega_z^2}{2e}(z^2 + \beta\rho^2), \quad (2)$$

where

$$\beta = \frac{\omega_p^2 - \frac{1}{2}\omega_z^2 - \omega_\phi^2}{\omega_z^2}. \quad (3)$$

Here,  $\omega_\phi$  accounts for a possible angular rotation frequency of the trapped plasma about the  $z$ -axis and this defocusing term usually equals zero for a linear Paul trap. We note that the meaning of  $\beta$  is nothing but the (resulting) radial to axial confinement force ratio.

Neglecting variations on an inter-particle scale, the density of a low temperature plasma (cold fluid) in a harmonic trap is constant and given by

$$n_0 = \frac{\epsilon_0}{e} \nabla^2 \Phi = \frac{2\epsilon_0 m \omega_z^2}{e^2} \left( \beta + \frac{1}{2} \right) = \frac{2\epsilon_0 m}{e^2} (\omega_p^2 - \omega_\phi^2), \quad (4)$$

independent of  $\omega_z$ . Furthermore, the shape of the cold plasma can be shown to be a spheroid [9] and is hence uniquely described through the length of the envelope semi-axes  $Z$  (along the trap axis) and  $R$  (in radial direction). The spheroid aspect ratio  $\alpha = Z/R$  and the  $\beta$ -parameter in Eq. (3) is related [9] as shown in Fig. 3(b).

<sup>2</sup> The current setup is restricted to emulate the quadrupole focusing/defocusing forces of a storage ring. For more involved experiments on crystalline beam emulation, one could look into the possibilities of implementing shear from bending by perturbing the crystals sideways with a suitable, periodic, transverse electric force.

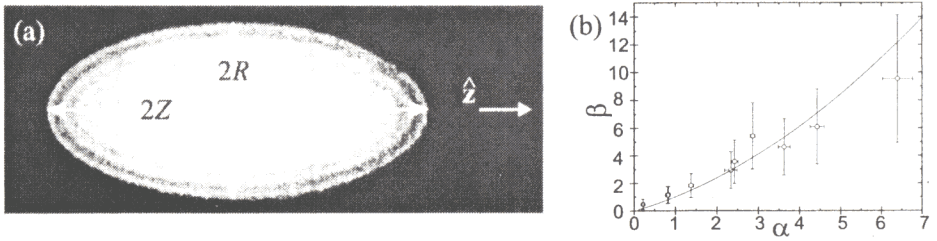


**FIGURE 3.** (a) Example of a Coulomb crystal with a shape and density described well by cold fluid theory with  $\omega_\phi = 0$ . The ions are arranged in closed spheroidal shells. (b) The relation between  $\alpha$  and  $\beta$  as given by cold fluid theory (line).  $\beta$  for a string-of-discs state crystal ( $\circ$ ) calculated from experimental parameters using Eq. (3) with  $\omega_\phi = 0.31 \times \omega_{rf}$ .

The shape of (non-rotating) Coulomb crystals in a linear Paul trap has previously been shown to be described well by cold fluid theory [10]. Figure 3(a) shows an image of such a crystal in the pulse-excited trap.

Bulk plasma oscillations in the cold fluid occur at the plasma frequency  $\omega_p = \sqrt{e^2 n_0 / \epsilon_0 m}$  which also equals the maximum bulk mode frequency in the case of a crystal [11]. From Eq. (4) we get  $\omega_p^2 = 2(\beta + 1)\omega_z^2 = 2(\omega_p^2 - \omega_\phi^2)$ . To avoid a 1:2 (parametric resonance) relationship between frequency of a bulk mode and the rf driving field we have the criterion  $2\omega_p < \omega_{rf}$ . This is equivalent to the tune condition for a crystalline ion beam as predicted by theory [12].

## RESULTS FROM EXPERIMENTS

In a recent series of experiments, we investigated the stability properties of laser cooled  $^{24}\text{Mg}^+$  Coulomb crystals when approaching the  $2\omega_p = \omega_{rf}$  resonance condition [13]. In this contribution, we shall only briefly summarize and discuss some of the results from this work. Notably, it was found that trapped crystals (initially in stable, closed shell configuration comparable to the one shown in Fig. 3) become unstable and blow up to a gaseous cloud state when the plasma frequency is increased to hit the parametric resonance. The plasma frequency was increased by increasing  $\omega_p$  through the rf waveform amplitude  $V_{rf}$ , while all other parameters were kept constant. The observed stability limit was in excellent agreement with the one predicted by theory and seemed quite insensitive to the axial confinement and the number of particles ( $\sim 50$ – $1000$ ). Surprisingly, the plasma was, however, observed to settle into a different and hitherto unobserved ordered structure when  $\omega_p$  was increased slightly above the value of instability (see Fig. 4). This final state has lower density and different spheroidal envelope than the initial closed shell structure observed just before hitting the point of instability, and appears as an axially ordered string of discs. By averaging over more frames we have, furthermore, seen indications of radial ordering within the discs (see Fig. 5).

As mentioned above, the initial closed shell structure shown in Fig. 4 is described well by cold fluid theory with the plasma in a non-rotating state. This cannot be the



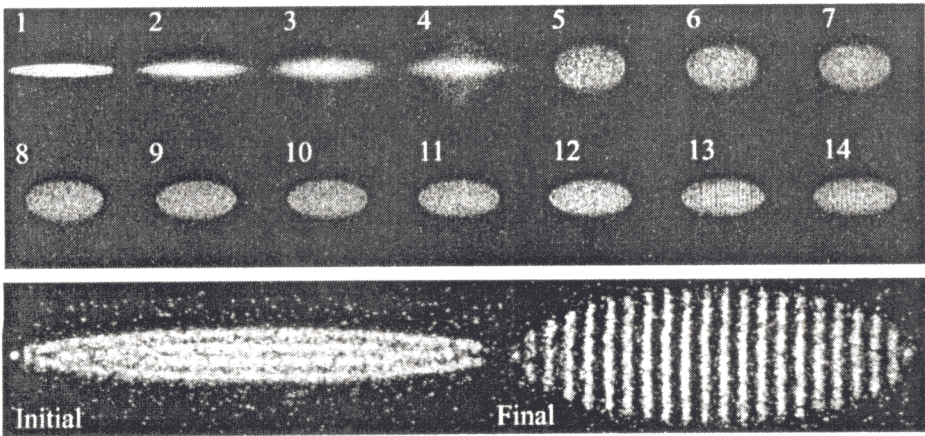


**FIGURE 4.** Upper part: Frame sequence (1-12) showing the closed shell→string-of-discs structural transition for about 370 ions when passing the parametric resonance  $2\omega_p = \omega_{rf}$ ; the sequence was acquired with 5 frames/s and the trap was operated at  $\omega_{rf} = 2\pi \times 700$  kHz with  $\tau = 0.14$ . Lower part: Close-up images of the initial and final state for the structural transition.

case for the final state as we only increase  $V_{rf}$  slightly to induce the structural transition so that  $\omega_p$  enters with approximately the same amount in the expressions for density and shape. Moreover, if one, anyway, considers a slight increase in  $\omega_p$ , this implies an increase both in density and aspect ratio, in contrast to the observations of the final state. However, the observed quantities might be explained from the cold fluid equations by assuming the plasma to be in a rotating state with  $\omega_\phi \neq 0$  [see, e.g., Eq. (4)]. This conjecture is supported by measurements performed on the string-of-discs state where  $\omega_z$  was varied and the corresponding aspect ratio was recorded [13]. By assuming the plasma to be rotating at the frequency  $\omega_\phi = 0.31 \times \omega_{rf}$ , we obtain the expected relation between  $\beta$  and  $\alpha$  as given by cold fluid theory [see Fig. 3(b)]. Otherwise (i.e., putting  $\omega_\phi = 0$ ),  $\beta$  calculated from Eq. (3) would be an order of magnitude off. A mechanism leading to rotation and which, furthermore, yields the assumed frequency is not clear at present.

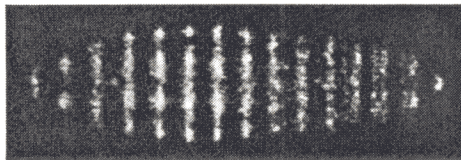


**FIGURE 5.** String-of-discs structure showing radial ordering. The image was obtained by averaging over 5 frames (=1 s).

## CONCLUSION AND DISCUSSION

In conclusion, we have investigated the stability of Coulomb crystals in a pulse-excited linear Paul trap having the same transverse dynamics as a storage ring with AG magnetic confinement. The observations agree well with current theory on crystalline plasmas and beams. Notably, it seems that the criterion  $2\omega_p < \omega_{rf}$  should be taken very seriously. However, at the stability limit we observed crystals to survive by rearranging in axially ordered structures. The observation was shown to be consistent with a string of rotating discs. We recently learned about some early work by Blümel *et al.* [14] where similar "layered structures" were found in connection with molecular dynamics simulations of up to 500 laser cooled ions in a conventional Paul trap. Why these simulations give rise to layered structures instead of ending up in a closed shell structure as found in equivalent work (see, e.g., [15] and references therein) is not clear at present. The possible and likely connection to our work will a subject of future studies.

## ACKNOWLEDGMENTS

This work was supported by the Danish National Research Foundation through Aarhus Center of Atomic Physics, the Danish Research Council, and the Carlsberg Foundation. N.K. gratefully thanks the organizing committee of the 2001 Workshop on Non-Neutral Plasmas for financial support.

## REFERENCES

1. Okamoto, H., and Tanaka, H., *Nucl. Instrum. Methods A*, **437**, 178 (1999).
2. Davidson, R. C., Qin, H., and Shvets, G., *Phys. Plasmas*, **7**, 1020 (2000).
3. Kjærgaard, N., and Drewsen, M., *Phys. Plasmas*, **8**, 1371 (2001).
4. Courant, E. D., Livingston, M. S., and Snyder, H. S., *Phys. Rev.*, **88**, 1190 (1952).
5. Christofilos, N. C., U. S. patent no. 2.736,799, filed March 10, 1950, issued February 28, 1956.
6. Bryant, P. J., in *Proceedings of the CERN Accelerator School: Fifth General Accelerator Physics Course*, edited by S. Turner, CERN 94-01, Geneva, 1994, vol. 1, p. 1.
7. Kjærgaard, N., *et al.*, *Appl. Phys. B*, **71**, 207 (2000).
8. Courant, E. D., and Snyder, H. S., *Ann. Phys.*, **3**, 1-48 (1958).
9. Dubin, D. H. E., *Phys. Rev. E*, **53**, 5268 (1996).
10. Drewsen, M. *et al.*, these Proceedings.
11. Dubin, D. H. E., and Schiffer, J. P., *Phys. Rev. E*, **53**, 5249 (1996).
12. Wei, J., Okamoto, H., and Sessler, A. M., *Phys. Rev. Lett.*, **80**, 2606 (1998).
13. Kjærgaard, N., Mølhave, K., and Drewsen, M., *Phys. Rev. Lett.* (2001), submitted.
14. Blümel, R., *et al.*, in *Proceedings of the 5th International Symposium on Quantum Optics*, Springer, 1989.
15. Schiffer, J. P., *et al.*, *Proc. Natl. Acad. Sci. U.S.A.*, **97**, 10697 (2000).